Examination of factors affecting strain tolerance of multifilament MgB_2 wires with Fe barrier

Hideki Tanaka[1], Motomune Kodama[1], Takaaki Suzuki[1], Hiroshi Kotaki[1], Gen Nishijima[2], Akiyoshi Matsumoto[2] and Michinaka Sugano[3]
[1]Research & Development Group, Hitachi, Ltd., 7-1-1 Omika-cho, Hitachi, Ibaraki, 319-1292, Japan
[2]National Institute for Materials Science, 1-2-1 Sengen, Tsukuba, Ibaraki, 305-0047, Japan
[3]High Energy Accelerator Research Organization (KEK), 1-1 Oho, Tsukuba, Ibaraki 305-0801, Japan
E-mail: hideki.tanaka.cj@hitachi.com

Received xxxxxx
Accepted for publication xxxxxx
Published xxxxxx

Abstract

There are two fabrication processes, the wind and react method and the react and wind method, to manufacture magnesium diboride (MgB_2) magnets. The react and wind method is desirable to simplify the coil fabrication process, but the understanding of strain tolerance of the sintered MgB_2 wire is insufficient. Hence, this study focused on determining the main factors that contribute to the strain tolerance of the MgB_2 wire with Fe barrier. It is generally thought that irreversible strain of sintered MgB_2 wire is mainly determined from the residual strain of MgB_2 filament, which is caused by the difference in the coefficient of thermal expansion among MgB_2 and metal sheaths. To estimate the residual strain of MgB_2 wire, the effect of yielded material must be considered. We calculated the residual strain of each constituent material used in the ten filaments MgB_2 wire in which copper was yielded during the cooling process from sintering temperature to room temperature. The calculated residual strains of metal sheaths except copper were compared with yield strains, and whether they yield was confirmed. The estimated residual strain of the MgB_2 filament was also compared with the experimentally obtained irreversible strain, and the difference in these strains suggests the strain tolerance of the MgB_2 filament. By measuring irreversible strains of the MgB_2 wires having different sintering times but the same residual strain, it was confirmed that the effect of the mechanical strength of the MgB_2 filament on the strain tolerance of the MgB_2 wire is slight but certain.

Keywords: MgB_2 wire, strain tolerance, residual strain, yield strain

1. Introduction

There are two methods for manufacturing magnesium diboride (MgB_2) coils: one is the wind and react method and the other is the react and wind method. During the coil-winding process with the react and wind method, quantification of the reversible strain limit of MgB_2 wires at room temperature (RT) is important to avoid degradation of the critical current (I_c) properties of MgB_2 coils. An I_c–external strain relation was evaluated as follows. I_c is proportional to the external strain in a reversible region, ±0.4%, and rapid and large degradation of I_c occurs in an irreversible region [1].

The irreversible external strain (ε_{irr}) of MgB_2 wire is generally determined from the residual strain (ε_r) of MgB_2 filament ($\varepsilon_{r,\ MgB2}$) [2], which is due to the difference in the coefficient of linear expansions among the MgB_2 filament and metal sheaths of MgB_2 wire. The ε_{irr} values of MgB_2 wires were measured in previous studies: Kováč *et al* evaluated ε_{irr} at 4.2 K of rectangular (ε_{irr}, 0.225–0.55%) [3] and circular (ε_{irr}, 0.304–0.900%) [4] cross-sections of MgB_2 wires having different constituent materials. Kodama *et al* measured the effect of constituent material fraction on ε_{irr} at RT in

multifilament MgB_2 wires (ε_{irr}, 0.30–0.65%) [5]. Tanaka *et al* showed ε_{irr} improvement by using stainless steel in the MgB_2 wire as the material having a large coefficient of linear expansion (ε_{irr}, 0.60%) [6]. The effect of sintering condition on I_c-external stress relation was confirmed by Yamamoto *et al* [7]. In that study, the irreversible external stress was compared among three sintering conditions of MgB_2/Fe wires, and the I_c degradation was observed at the same stress level. ε_r is determined from the difference in temperature between sintering and evaluation temperature, so ε_{irr} of MgB_2 wires should change not only due to sintering temperature but also evaluation temperature. Alknes *et al* evaluated the ε_{irr} of MgB_2 wires at 77 K and RT and found that ε_{irr}, 0.35%, at 77 K was larger than that, 0.25%, at RT [8]. Irreversible external-stress also changes due to evaluated temperature because stress-strain (SS) curves of MgB_2 wires have dependence on evaluated temperature, as shown in previous studies [9, 10].

In the above studies, the effect of mechanical strength of MgB_2 filament on ε_{irr} was not mentioned. Kováč *et al* suggested the possibility of this effect by comparing the ε_{irr} of in-situ and ex-situ MgB_2 wires (highest ε_{irr}, 0.90%) [10]. Tanaka *et al* also investigated this effect by comparing the ε_{irr} of MgB_2 wires having different sintering conditions (ε_{irr}, from 0.25% to 0.30–0.34%) [11]. The experimental results of the above studies qualitatively indicated that ε_{irr} of MgB_2 wires is affected by $\varepsilon_{r,\,MgB2}$. If there is no yield on metal sheaths of MgB_2 wires during the cooling process from sintering temperature to evaluated temperature, $\varepsilon_{r,MgB2}$ can be roughly calculated. A quantitative comparison between measured ε_{irr} and calculated $\varepsilon_{r,\,MgB2}$ of various MgB_2 wires without considering the yield was conducted by Kováč *et al*, but there was a 0.2% (2,000 με) strain's gap between them [2]. As shown in later section, there are a strain's difference of 0.04% (400 με) between calculated values of $\varepsilon_{r,\,MgB2}$ with or without considering the yield of constituent materials, so the effect of the yield can be thought as one of the reasons of the gap in the previous work.

We calculated the residual strains of constituent materials of a MgB_2 wire by considering whether metal sheaths yield. It is well known that Cu has low yield strain, so it is easily yielded due to the residual strain. However, the yield strains of Fe and Monel annealed at sintering temperature for MgB_2 wire must be compared with their residual strains caused by cooling from sintering temperature to RT. The yield and residual strains of metal materials were experimentally measured and calculated, respectively. The different values of yield and residual strains were also confirmed by comparing to yield points of the SS curves of MgB_2 wires sintered at different sintering times.

2. Methods

Figure 1 shows cross-sections of the MgB_2 sample wires used in this study sintered at 600°C for (a) 12 hr, (b) 48 hr and 96 hr (not shown). These wires were sampled from a 1.52-mm wire with Fe barrier sheaths, a Cu rod, and Monel outer sheath, so the sintering time is the only difference between these samples. The manufacturing process of this 1.52-mm wire was given in a previous study [12]. Since these sample wires before sintering had a gentle bend, they were loaded into a straight stainless-steel tube then sintered to straighten them. In this 1.52-mm wire, the sintering condition of 600°C for 12 hr is the best condition for maximizing I_c at 10–20 K.

The tensile strain was applied to the MgB_2 sample wires by uniaxial tensile tests as follows. The sample length was 100 mm, and two strain gauges (FBY-06, Tokyo Measuring Instruments Laboratory Co., Ltd) were mounted in the centre of each sample facing each other as shown in Figure 6 (b) in the reference paper [6] with using the adhesive for strain gauges. (CN, Tokyo Measuring Instruments Laboratory Co., Ltd). Even for non-straight samples, averaging the strains measured using two strain gauges makes it easier to evaluate

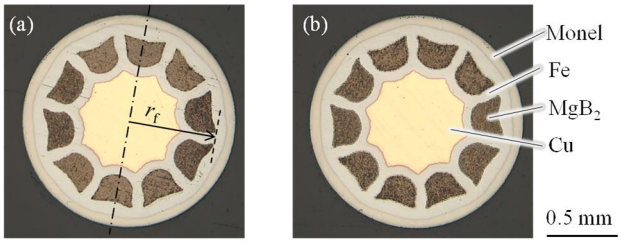

Figure 1. Cross-sections of 10-filament MgB_2 wires sintered at 600°C for (a) 12 hr and (b) 48 hr. The cross-section for 96 hr was omitted, because it is similar to the one for 48 hr. Dash-dot line in (a) shows an example of a neutral line of bending. Area fractions of MgB_2, Fe, Cu, and Monel were 25.6%, 37.1%, 20.5%, and 16.8%, respectively.

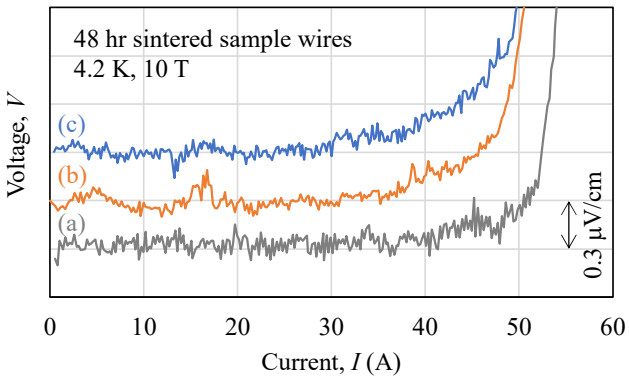

Figure 2. *V-I* curves of 48 hr sintered (a) sample wire without external strain, (b) tensioned sample wire ,and (c) bent sample wire. Maximum applied strains to MgB_2 filament of (b) and (c) are 0.26% and 0.27%, respectively. Measured I_c values of sample wires (a), (b) and (c) are 50.7 A, 45.4 A and 44.6 A, respectively.

the strain immediately after the start of the tensile test. The strain-gauge length (strain direction, longitudinal direction of sample) was 0.6 mm and width was 0.8 mm. Since strain gauge is glued to thin round samples, such a narrow strain gauge was used for our study. According to the instruction manual of the strain gauge, by attaching half the width of the strain gauge to a sample, measurement error can be suppressed to within 10%. Even though it is a visual confirmation, considering that more than half of the gauge section area was attached to the each sample, it can be assumed that the measurement error of strain is less than 10%.

In this paper, we assess the axial strain up to a maximum of 0.3% (3,000 με) and utilize this as an example to calculate measurement error. When the length of a cylinder with constant volume increases by 0.3%, the change in circumference is $1 - (1 - 0.3\%)^{0.5}$. The gauge factors in the sample length direction and circumferential direction of the strain gauge are 2.18% and 1.3%, respectively. Hence, the measurement error when measuring a strain of 0.3% is $[\{1 - (1 - 0.3\%)^{0.5}\} \times 1.3\%] / (0.3\% \times 2.18\%) = 3\%$. (It means 3,000 με × 3% = 90 με.) This magnitude is smaller than the error of 10% in the case of a risk with a small adhesive area of the strain gauge. The circumferential gauge factor of the strain gauge CEFLA-3, which will be used later, is 0.7%, and the measurement error will be even smaller.

For the tensile test, an autograph (AG-100kNX, SHIMADZU CORPORATION) was used to apply the tensile force to the sample wires. The tensile force was increased at the strain ratio 1–2 × 10^{-6} s^{-1} while observing the response of the strain gauges, and the tensile force was unloaded when the desired strain was reached. By repeating tensile tests, the sample wires with different maximum applied tensile strains were prepared. The strain gauges were removed before I_c measurement, but voltage taps were installed at 5-mm intervals so that the place where the strain gauges were attached became the evaluation part of I_c.

Bending strain was also applied to the sample wires through bending tests as follows. Various bending strains were applied to the sintered sample wires by using various bobbins of different diameters. The outer radius of the bobbin ranged from 400 to 165 mm. The sample wires were bent with several bobbins, and bending and releasing were repeated three times at RT. The number of bends of three times simulates the insulation process and the coil winding process, and the bending direction is the same direction. The maximum applied strain to the MgB_2 filament by bending is expressed as $r_f / (r_b + r_w)$, where r_f is the radius of the outer circle of the filament area as shown in Figure 1, r_b is the outer radius of the bobbin used for bending, and r_w is the radius of the sample wire. There are errors of 2% in the applied strain by bending due to variations in r_f.

The I_cs of the sample wires were measured by the typical four-probe method. The sample wire temperature was decreased to 4.2 K with liquid helium and to 10–20 K with gas helium. The sample length was 40 mm, distance between voltage taps was 5 mm. While measuring I_c, the sample wires are subjected to an external magnetic field, and the Lorentz force acts in the direction of the wire radius and is supported by the sample holder. Hence, the Lorentz force does not affect the strain tolerance of sample wires. Criterion of the electric field was 0.3 μV/cm. The general standard is 1.0 μV/cm, but it was set strictly to clearly determine the I_c degradation due to the applied strain. Figure 2 shows the representative *V-I* curves of a sample wire without I_c degradation and tensioned or bent sample wires with I_c degradations.

Nine round metal rods for measuring SS curves were processed from each metal and annealed, and their SS curves were obtained from uniaxial tensile tests. The measurement method of SS curves was the same as the uniaxial tensile test mentioned above for the MgB_2 sample wires, but strain gauges (CEFLA-3, Tokyo Measuring Instruments Laboratory Co., Ltd, 3.0 mm in length, 0.6 mm in width) were used for the metal rods. Table 1 shows the properties of the metal rods. Figure 3 shows the measurement results of the SS curves of each metal rod. Discontinuous yielding of Fe and continuous yielding of Cu and Monel were observed. There was a noisy signal near the yield point of Fe, which is an effect of the Luders band propagation. It is understood that Luders band propagates from the chuck area towards the center. During this measurement, the iron rod closer to the chuck area than the strain gauge temporarily elongates before the propagation reaches the area where the strain gauge is attached. Consequently, the iron rod at the area where the strain gauge is attached temporarily contracts, resulting in the occurrence of noisy signal.

An SS curve can be approximated by two straight lines connected at a point called “tentative yield point”, and approximated young’s modulus (E), yield strain (ε_y), and coefficient of work hardening (K) are given for each metal rod, as shown in Table 1. As shown in Figure 3(c), there is a

Table 1. Young’s moduli, E, yield strain, ε_y and coefficient of work hardening, K obtained from uniaxial tensile tests of metal rods.

Metal	Diameter (mm)	Sintering time (hr)	Fitting parameters		
			E (GPa)	ε_y (%)	K (GPa)
Fe	1.5	12	213	0.13	0
		48	212	0.12	0
		96	210	0.105	0
Monel	1.8	12	179	0.16	0
		48	173	0.15	0
		96	175	0.14	0
Cu	3.8	12	112	0.021	4.0
		48	106	0.018	3.8
		96	110	0.018	3.8

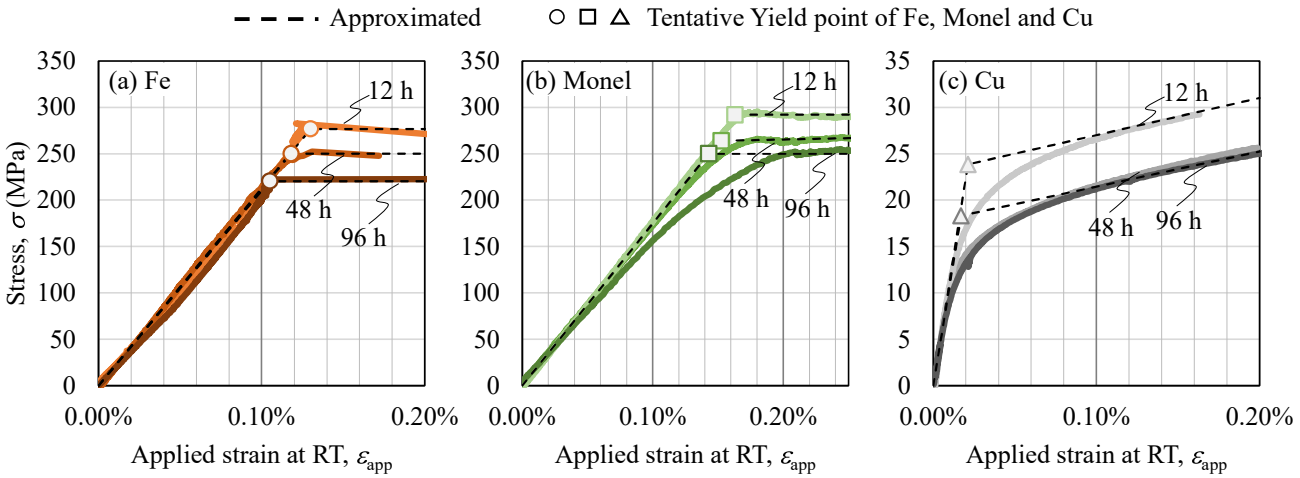

Figure 3. Stress-strain curves measured from (a) Fe, (b) Monel and (c) Cu sample rods annealed at 600°C for 12, 48 and 96 hr. Broken line shows approximated curve, which can be drawn using E, ε_y, and K listed in Table 1. Open circles (Fe), squares (Monel), and triangles (Cu) show tentative yield points of each metal rod.

significant difference between the measured curves and the approximate curves in Cu. When the internal strain of Cu is less than 0.1%, there is a large error when referring to stress and strain.

3. Results

Figures 4 and 5 show the I_c measurement results of the tensioned and bent sample wires, respectively. The horizontal axis is the maximum strain applied to MgB_2 filament by tension or bending at RT, and the vertical axis is the normalized I_c divided by the averaged I_cs of the two sample wires without external strain. Two other sample wires were bent and evaluated for each ε_{app}, except for the strain condition in which clear I_c degradation was observed. Due to the variation in r_f, the magnitude of the strain applied to the filaments differs even for samples with the same bending radius. To ensure reproducibility, it was necessary to measure two sample wires each. The variation of I_c in these MgB_2 wires is normally about ±7% [13], and the criteria of I_c degradation was defined as I_c that falls below 90% or decreases rapidly in response to the increase in ε_{app}. As shown in Figures 4 and 5, in the sample wires sintered for 12 hr, I_c degradation occurred within 0.20–0.22% and 0.20–0.24% of ε_{app}, respectively. Since these results were almost identical, it was determined that I_c degradation of the 12-hr sintered sample wires occurred within the applied strain range of 0.20–0.22%. As shown in Figures 4 and 5, however, I_c degradations of the 48-hr and 96-hr sintered sample wires were observed within 0.24–0.26% and 0.26–0.28%, respectively. These ranges are 0.04% and 0.06% higher strain compared with that of the 12-hr sintered sample wires.

Figure 6 shows the I_c measurement results of the sintered sample wires without applying mechanical load. The I_cs were

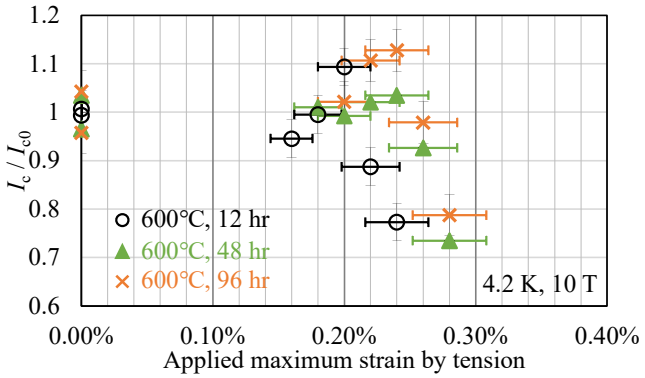

Figure 4. Normalized I_c obtained from tensioned sample wires as function of applied maximum strain at RT. Strain-measurement error determined from strain gauges was smaller than 10%.

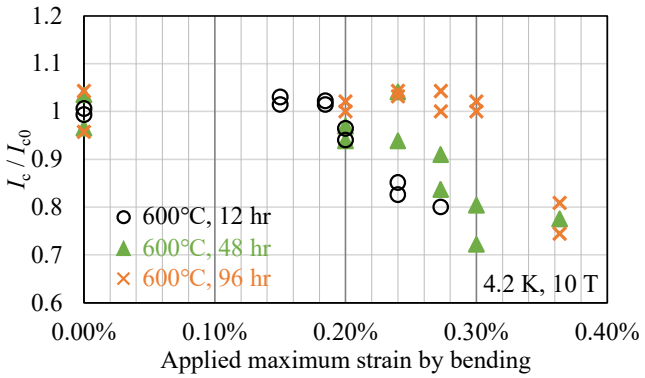

Figure 5. Normalized I_c obtained from bent sample wires as function of applied maximum strain at RT. Applied strain error due to the deviation of r_f was smaller than 2%.

higher in the 12-hr sintered sample wire, and the I_cs in the 48-hr and 96-hr sintered sample wires ranged from 50 to 80% compared with that in the 12-hr sintered sample wire. The main pinning centre of MgB_2 wire is generally the grain boundaries of MgB_2 [14]. Therefore, a main reason of I_c reduction by prolonged sintering time is thought to be the reduction of the pinning centre. The increasing sintering time increases the grain size of MgB_2, and the density of the grain boundary in MgB_2 filament is reduced. It is considered that un-reacted magnesium and boron powders are one of the pinning centres. Even in MgB_2 filament sintered at 600°C for 24 hr, there are un-reacted powders [15]. Therefore, the density of the un-reacted powders and the pinning centre in the 48-hr and 96-hr sintered filament are thought to be lower than that of the 12-hr sintered filament. With the above considerations, it is thought that the mechanical strength of 48-hr and 96-hr sintered MgB_2 filament are higher than that of 12-hr sintered filament.

4. Discussion

The strain tolerance of MgB_2 wire is mainly determined from the residual strain applied to the MgB_2 filament ($\varepsilon_{r,\,MgB2}$) during cooling after sintering [2]. The internal strain (ε_{int}) of the MgB_2 filament is assumed zero when MgB_2 is reacted from the mixed powder state of magnesium and boron powders at the sintering temperature of 600°C, because constituent materials except MgB_2 are stress relieved at 600°C as follows: 600°C is sufficiently high for recrystallization on plastically deformed Cu. According to a previous study [16], heat-treatment at 600°C for 40 min can recrystallize Fe (working ratio 60%), and yield stress depends on grain size. Regarding Monel, 538–566°C is for stress-relieving temperature, and 704–982°C is for recrystallization temperature [17]. Therefore, 600°C annealed Monel is stress relieved but has uncertainty for recrystallization.

The linear expansion coefficients of metallic materials are generally larger than that of the MgB_2 filament, so compressive strain remains in the MgB_2 filament after cooling. Sugano *et al* calculated the ε_r on Bi2223 wire that includes yielded metal (Ag) sheaths [18] and it was come from an original reference [19]. According to this previous study, the residual strain of component i at temperature $T = T'$ is expressed as

$$\varepsilon_{r,\,i} = \int_{T_A}^{T'} \{\alpha_c(T) - \alpha_i(T)\}\,dT, \qquad (1)$$

where $\alpha_c(T)$ and $\alpha_i(T)$ are the coefficient of thermal expansion of the composite wire and each component, respectively, and T_A is sintering temperature. The components of the MgB_2 wire are MgB_2, Fe, Cu, and Monel. The yield stress and strain of Cu is approximately 20 MPa and 0.02%, respectively. It indicates that Cu will soon yield after cooling starts from 600°C. Therfore, the temperature integral of $\alpha_c(T)$ after Cu yields is calculated with using equation (2), then ε_r of each constituent material is obtained from equaion (1) with considering Cu yields. Where j is MgB_2, Fe, and Monel, E_j (T ') and V_j are young's modulus and area fraction of each component, $\sigma_{y,Cu}(T')$ and $\varepsilon_{y,Cu}(T')$ are yield stress and strain of Cu, and $K_{Cu}(T')$ is coefficient of work hardening of Cu [18]. In this paper, the V_js from 600°C to RT is assumed to be equal to those at RT (values are shown in the caption of Figure 1). As shown in equation (2), yield stress (σ_y), yield strain (ε_y), and coefficient of work hardening (K) of constituent metals are required to estimate ε_r.

Figure 7 shows the temperature dependencies of E used in this study. The measurement results of E of each material listed in Table 1 were applied to the value of each material at

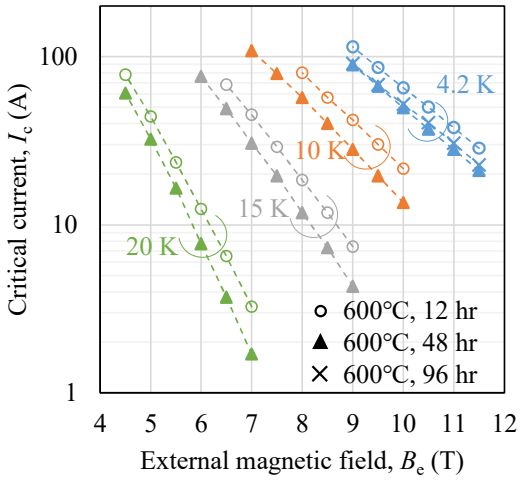

Figure 6. I_c-B_e-T properties obtained from MgB_2 sample wires sintered at 600°C for 12 hr, 48 hr and 96 hr.

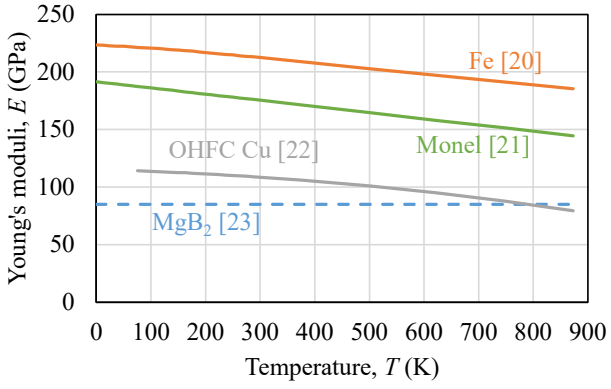

Figure 7. Young's modulus of constituent materials of MgB_2 wire as function of temperature.

$$\int_{T_A}^{T'} \alpha_c(T)\,dT = \frac{\sum_j \int_{T_A}^{T'} \alpha_j(T)dT\, E_j(T')V_j + \left[-\sigma_{y,Cu}(T') + \left\{\int_{T_A}^{T'} \alpha_{Cu}(T)dT - \varepsilon_{y,Cu}(T')\right\} K_{Cu}(T')\right] V_{Cu}}{\sum_j E_j(T')V_j + K_{Cu}(T')V_{Cu}} \qquad (2)$$

RT, and the temperature-dependent slopes of each material were based on those in previous studies [20, 21, 22]. Since Young's modulus of MgB_2 was found only at RT [23], it was assumed that there is no temperature dependence, shown as a dashed line in the figure. Neglecting the temperature dependence when estimating ε_r leads to an error. Hence, incorporating it into the estimation poses a challenge that should be addressed in the future. Figure 8 shows the coefficient of linear expansion given in previous studies [5, 24, 25]. The temperature dependence of MgB_2 is shown as an extrapolated dashed line in the log function because there was no value above RT.

The residual strains of the MgB_2 filaments at RT were calculated and compared with the measured strain tolerance of the MgB_2 wires. Figure 9 shows the calculated ε_{int}s of the constituent materials of the MgB_2 sample wires sintered at 600°C for 12 hr and cooled to 15°C. The horizontal axis is temperature, and vertical axis is the ε_{int} of each material. All ε_{int}s were assumed to zero at 600°C because metal materials accepted stress-relieving annealing at 600°C and because MgB_2 grains were sintered at that temperature. As the yielding condition of Cu, the measured tentative yield point of the 12-hr sintered Cu rod was used for this calculation. The ε_{int} of Cu during the cooling process crossed over $\varepsilon_{y,\,Cu}$ (= 0.02%) near 600°C then reached 0.26% at RT. The residual strains of Fe ($\varepsilon_{r,\,Fe}$) and Monel ($\varepsilon_{r,\,Monel}$) at RT were 0.01% and 0.09%, and were lower than the yielding conditions at RT, $\varepsilon_{y,\,Fe}$ = 0.13% and $\varepsilon_{y,\,Monel}$ = 0.16%, respectively. Regarding 48-hr sintering, the yield strain of Cu was slightly smaller than that for 12-hr as shown in Table 1, and the $\varepsilon_{r,\,Cu}$, $\varepsilon_{r,\,Fe}$, and $\varepsilon_{r,\,Monel}$ at RT were 0.26%, 0.01%, and 0.09%, respectively. The calculated residual strains of constituent materials after 48-hr sintering were almost the same as those of 12-hr sintering.

In the previous discussion, we utilized the measured values of the yield point at room temperature. However, in actuality, the yield stress and strain are influenced by temperature. In the case of annealed Cu, it has been mentioned that the yield stress decreases as the temperature increases [26]. Therefore, similar to our previous discussion, it can be confirmed that Cu starts yielding as soon as the cooling process begins from 600°C. The temperature dependence of the yield stress of Fe and Monel was investigated by the references [27, 28]. The temperature dependence of the Young's modulus, as shown in Figure 7, was used to convert them into yield strains, as shown in Figure 9. It was found that both Fe and Monel do not yield within the temperature range under consideration. This means that the yielded material during cooling after 600°C sintering is only Cu. Therefore, it can be said that the prolongation of sintering time affects the yield conditions of metal materials but does not meaningfully affect the residual strains at RT. Here, the ε_{int}s of each material in Figure 9 above 350°C include errorness due to the rough approximation of the SS curve of Cu.

Here, quantitatively assess the influence of taking into account the yield of Cu on the $\varepsilon_{r,\,MgB2}$ at RT. As shown in Figure 9, $\varepsilon_{r,\,MgB2}$ at RT was -0.18% when considering the yield of Cu. On the other hand, assuming that Cu does not yield, the calculated $\varepsilon_{r,\,MgB2}$ at RT using equation (2) was -0.22%. Therefore, the yield of Cu had a 0.04% (400 με) impact on the

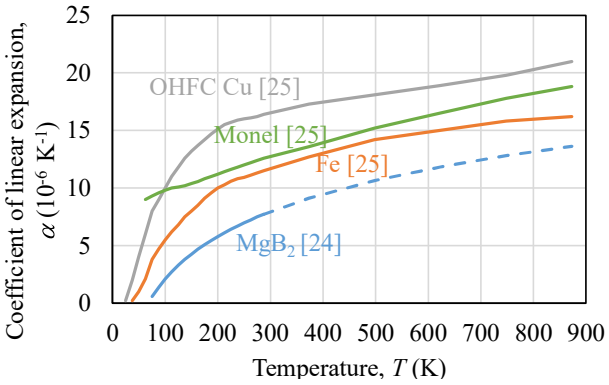

Figure 8. Coefficient of linear expansion of constituent materials of the MgB_2 wire as function of temperature

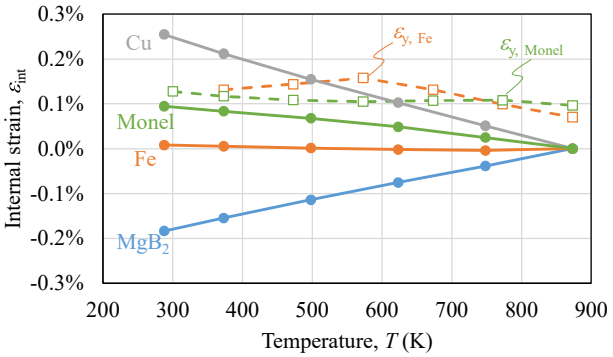

Figure 9. Calculated internal strain changes of constituent materials of the MgB_2 wire during cooling process from sintering temperature to RT. The open symbols are the calculated yield strain of Fe and Monel.

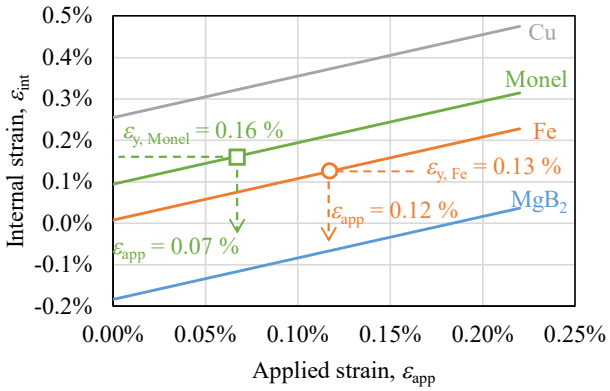

Figure 10. Calculated internal strains of constituent materials of the MgB_2 wire sintered for 12 hr as function of applied strain at RT.

$\varepsilon_{r,\,MgB2}$ at RT and the magnitude of this impact is so significant that it cannot be disregarded.

The estimated residual strains of MgB_2, Fe, Monel, and Cu at RT were -0.18%, 0.01%, 0.09%, and 0.26%, respectively, as shown in Figure 9. The validity of this estimation can be confirmed by comparing measured and calculated SS curves of the MgB_2 wires as follows. During measurement of SS curves of the MgB_2 wires, it was assumed that the ε_{app} of each constituent material is the same as the strain applied to the wires. Figure 10 shows the relations between the ε_{int}s of the constituent materials and ε_{app} at RT. The ε_{int} values were obtained by adding the ε_{app} to the ε_{int} at RT. As mentioned previously, Cu yielded without the applied strain. The $\varepsilon_{y,\,Fe}$ and $\varepsilon_{y,\,Monel}$ in Table 1 are also plotted in Figure 10. The applied strains at tentative yield points of Fe and Monel obtained from the difference between the measured ε_y and calculated ε_r of each material were 0.12% and 0.07% for 12-hr sintering and 0.11% and 0.06% for 48-hr sintering, respectively. These applied strains should agree with the yield points of SS curves of the MgB_2 wires. Figure 11 shows the measured and estimated SS curves of the MgB_2 wires sintered at 600°C for 12, 48 and 96 hr. The slopes of estimated lines were obtained from the area fractions and the E as non-yielded or the K as yielded of each constituent material. The estimated curves agreed well with the measured curves in the area before the yield point of Fe, confirming the validity of the residual-strain calculations of the constituent materials at RT. The measured yield strains of Fe in the MgB_2 wire were slightly larger than the estimated ones, so the yield strain of Fe in the MgB_2 wires was slightly larger than that in the Fe rod. The main reason for this difference is thought to be the difference in the Fe grain size between the MgB_2 wires and the Fe rod because re-crystalized Fe has grain-size dependency on the yield strain [16]. The difference in the Fe grain size between the MgB_2 wire and Fe rod is shown in Figure 12. These optical microscopic images were obtained after chemical etching, and the grain sizes of Fe in the MgB_2 wire were smaller than those in the Fe rod.

In the area of after yield of Fe, estimated SS curves had a certain gradient due to E of MgB_2, but the measured SS curves were or began to be flat. These flattened SS curves may suggest the plastic deformation of the Fe sheaths known as the Luders band propagation, and it may lead to cracks in the MgB_2 filament. From this assumption, if the strain applied to the MgB_2 wire is larger than the yield point of Fe, the I_c of the wire should degrade. Within the range of measurement results in this study, there was a specific strain range where there was no degradation of I_c, even when the SS curve was flat. To examine the details of these flattened SS curves, tests with the Fe sheathed mono-core MgB_2 wires will be effective. Estimation methods of the residual and yield strains of Fe shown in this study will also be important.

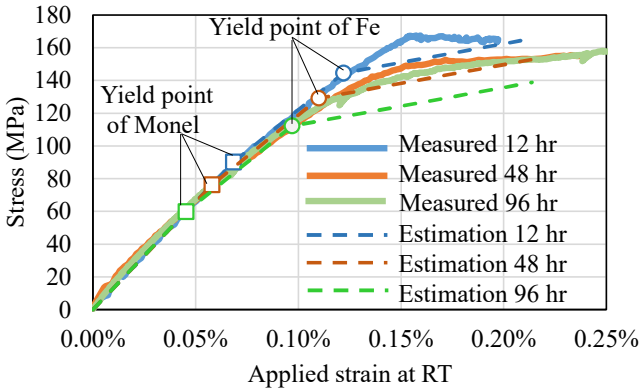

Figure 11. Comparison of measured and estimated stress-strain curves of each sintering condition. The maximum applied strain of measured SS curves are 0.20%, 0.24% and 0.28% at 12, 48 and 96 hr sintered sample wires, respectively. Yield points of Monel and Fe on estimated SS curves were calculated from residual strains shown in Figure 10.

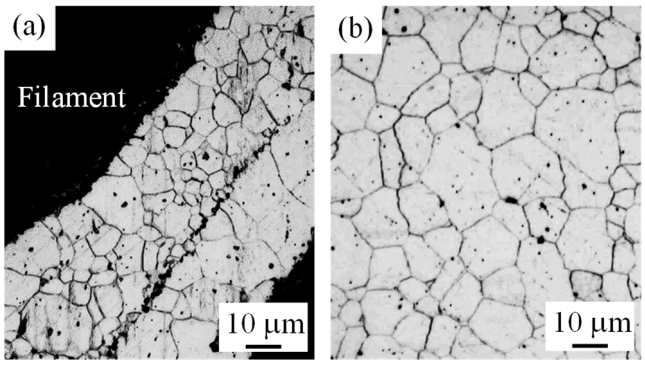

Figure 12. Optical microscopic images of (a) MgB_2 wire and (b) Fe rod sintered at 600°C for 12 hr. Both cross sections were chemically etched using nitric acid to highlight edges of Fe grains.

The strain tolerances of MgB_2 filaments at RT are determined by the sum of the ε_{irr} and the $\varepsilon_{r,\,MgB2}$, and they are 0.02–0.04%, 0.06–0.08% and 0.08–0.10% of 12, 48 and 96-hr sintered MgB_2 wires, respectively. It means that the prolongation of sintering time enhanced the strain tolerance of MgB_2 filaments. The strain tolerance of the MgB_2 wire was enhanced from 0.20–0.22% to 0.24–0.26% and 0.26–0.28% by the prolongation of sintering time, and the difference of them were 0.04% and 0.06%. When manufacturing MgB_2 magnets, the higher strain tolerance leads to the reduced allowable bending radius. Even though I_c of longer sintered wire is lower than the best performance of the wire, the ease of handling MgB_2 wire is highly valuable, especially for applied devices used in self-magnetic fields such as power cables, and magnets with relatively low magnetic field strength, such as magnets for the beam focusing magnet.

5. Conclusion

To clarify the mechanism of strain tolerance of MgB_2 wire, the residual and yield strains of constituent materials of the sample wires were calculated and compared with experimental values. The results of this study are summarized as follows. (1) It was confirmed that Cu was the only yielded material during the cooling process from sintering to room temperatures for MgB_2 sample wires sintered at 600°C for 12, 48 and 96 hr. This suggests that the residual compressive strain of the MgB_2 filament is not significantly affected by sintering time. (2) The validity of the residual-strain calculations of Fe and Monel was confirmed using the yield points of the SS curves of three MgB_2 sample wires sintered at different sintering times. (3) The irreversible strain at room temperature of the MgB_2 sample wires sintered at 600°C for 12, 48 and 96 hr were 0.20–0.22%, 0.24–0.26% and 0.26–0.28%, respectively, so the prolongation of sintering time slightly enhanced the strain tolerances of MgB_2 filaments and wires. (4) The critical current of 48 and 96 hr sintered sample wires degraded compared with that of the 12 hr sintered sample wire. It is thought that by increasing the sintering time, the unreacted powders and pinning centres decrease, but the strength of the filament improves.

5. References

[1] Kitaguchi H, Matsumoto A, Hatakeyama H and Kumakura H 2003 *Supercond. Sci. Technol.* **16** 976-979

[2] Kováč P, Dhallé M, Melišek T, van Eck H J N, Wessel W A J, ten Haken B and Hušek I 2003 *Supercond. Sci. Technol.* **16** 600-607

[3] Kováč P, Melišek T, Kopera L, Hušek I, Polak M and Kulich M 2009 *Supercond. Sci. Technol.* **22** 075026

[4] KováčP, Kopera L, Melišek T, Rindfleisch M, Haessler W and Hušek I 2013 *Supercond. Sci. Technol.* **26** 105028

[5] Kodama M, Kotaki H, Suzuki T and Tanaka H 2022 *Supercond. Sci. Technol.* **35** 094007

[6] Tanaka H, Suzuki T, Kodama M, Kotaki H, Nishijima G and Matsumoto A 2022 *IEEE Trans. Appl. Supercond.* **32** 6200205

[7] Yamamoto K, Osamura K, Balamurugan S, Nakamura T, Hoshino T and Muta I 2003 *Supercond. Sci. Technol.* **16** 1052-1058

[8] Alknes P, Hagner M, Bjoerstad R, Scheuerlein C, Bordini B, Sugano M, Hudspeth J and Ballarino A 2016 *IEEE Trans. Appl. Supercond.* **26** 8401205

[9] Dhakarwal M, Ogitsu T, Sugano M, Tanaka H and Watanabe H 2019 *IEEE Trans. Appl. Supercond.* **29** 4802404

[10] Kováč P and Kopera L 2012 *IEEE Trans. Appl. Supercond.* **22** 8400106

[11] Tanaka H, Suzuki T, Kodama M, Nishijima G and Matsumoto A 2019 *IEEE Trans. Appl. Supercond.* **29** 8401104

[12] Tanaka H, Kodama M, Ichiki Y, Kusunoki T, Kotaki H, Suzuki T, Nishi K and Okamoto K 2017 *IEEE Trans. Appl. Supercond.* **27** 4600904

[13] Tanaka H, Suzuki T, Kodama M, Koga T, Watanabe H, Yamamoto A and Michizono S 2020 *IEEE Trans. Appl. Supercond.* **30** 6200105

[14] Kodama M, Ichiki Y, Tanaka K, Okamoto K, Yamamoto A and Shimoyama J 2014 *Supercond. Sci. Technol.* **27** 055003

[15] Kodama M, Suzuki T, Tanaka H, Okishiro K, Okamoto K, Nishijima G, Matsumoto A, Yamamoto A, Shimoyama J and Kishio K 2017 *Supercond. Sci. Technol.* **30** 044006

[16] Sakui S and Sakai T 1972 Tetsu-to-Hagane **58** 1438-1455

[17] Monel 400 Tech Data (hightempmetals.com) https://www.hightempmetals.com/techdata/hitempMonel400data.php

[18] Sugano M, Osamura K and Nyilas A 2004 *Physica C* **412-414** 1114-1119

[19] Ochiai S, Hayashi K, Osamura K 1990 *J. Mater. Sci.* **25** 3467-3474

[20] Cryogenics and Superconductivity Society of Japan, *Choudendo Teionkougaku Handobukku* (Handbook of Superconductivity and Cryogenics) (Ohmsha, Tokyo, 1993) [in Japanese].

[21] The Engineering ToolBox https://www.engineeringtoolbox.com/young-modulus-d_773.html

[22] Copper Alloys Knowledge Base http://www.conductivity-app.org/alloy-sheet/31

[23] Sugano M, Ballarino A, Bartova B, Bjoerstad R, Gerardin A and Scheuerlein C 2016 *Supercond. Sci. Technol.* **29** 025009

[24] Neumeier J J, Tomita T, Debessai M, Schilling J S,Barnes P W, Hinks D G and Jorgensen J D 2005 *Phys. Rev.B* **72** 220505

[25] Touloukian Y S, Kirby R K, Taylor R E and Desai P D 1975 *Thermal Expansion Metallic Elements and Alloys*(Thermophysical Properties of Matter, The TPRC DataSeries vol 12) Purdue University

[26] Sia Nemat-Nasser and Yulong Li 1998 *Acta mater* **46** pp 565-577

[27] Guosheng Su, Yi Liu, Xiaodong Xiao, Jin Du, Peirong Zhang, and Xuehui Shen 2021 *JMEPEG* **30** 2036-2046

[28] Austral Wright Metals https://www.australwright.com.au/alloys-datasheet/